

Article

## Applicability of Green-Red Vegetation Index for Remote Sensing of Vegetation Phenology

Takeshi Motohka <sup>1,\*</sup>, Kenlo Nishida Nasahara <sup>1</sup>, Hiroyuki Oguma <sup>2</sup> and Satoshi Tsuchida <sup>3</sup>

<sup>1</sup> Graduate School of Life and Environment Sciences, University of Tsukuba, 1-1-1 Tennoudai, Tsukuba, Ibaraki 305-8572, Japan; E-Mail: kenlo@sakura.cc.tsukuba.ac.jp

<sup>2</sup> National Institute for Environmental Studies, 16-2 Onogawa, Tsukuba, Ibaraki 305-8506, Japan; E-Mail: oguma@nies.go.jp

<sup>3</sup> National Institute of Advanced Industrial Science and Technology, 1-1-1 Umezono, Tsukuba, Ibaraki 305-8568, Japan; E-Mail: s.tsuchida@aist.go.jp

\* Author to whom correspondence should be addressed; E-Mail: takeshi.motooka@gmail.com; Tel.: +81-29-853-4897; Fax: +81-29-853-4897.

Received: 25 August 2010; in revised form: 26 September 2010 / Accepted: 9 October 2010 /

Published: 15 October 2010

---

**Abstract:** We evaluated the use of the Green-Red Vegetation Index (GRVI) as a phenological indicator based on multiyear stand-level observations of spectral reflectance and phenology at several representative ecosystems in Japan. The results showed the relationships between GRVI values and the seasonal change of vegetation and ground surface with high temporal resolution. We found that GRVI has the following advantages as a phenological indicator: (1) “GRVI = 0” can be a site-independent single threshold for detection of the early phase of leaf green-up and the middle phase of autumn coloring, and (2) GRVI can show a distinct response to subtle disturbance and the difference of ecosystem types.

**Keywords:** phenology; remote sensing; spectral reflectance; digital camera; Green-Red Vegetation Index; phenological eyes network

---

## 1. Introduction

Remote sensing is an effective approach for tracking phenological changes such as leaf green-up and autumn coloring from the regional to the global scale [1]. In fact, time-series datasets of spectral indices obtained by satellite remote sensing have demonstrated its usefulness in detecting the earlier shift in spring phenology on a regional scale [2–7], understanding the phenological response to meteorological conditions and developing a prognostic leaf onset model [8,9], and classifying vegetation types [10].

The Normalized Difference Vegetation Index (NDVI), which is a normalized ratio of red and near-infrared reflectance [11], has been used in many phenological studies, including the detection of timing of leaf green-up and autumn coloring [12]. NDVI is defined as follows:

$$NDVI = \frac{\rho_{nir} - \rho_{red}}{\rho_{nir} + \rho_{red}} \quad (1)$$

where  $\rho_{red}$  and  $\rho_{nir}$  are reflectance of visible red and near-infrared, respectively. However, according to the results of time-series ground observation of the spectral indices and seasonal changes of a forest canopy, the conditions of the canopy in autumn indicated by NDVI are not identical among years; therefore, it is difficult to monitor leaf autumn coloring by using time-series NDVI [13]. One simple and possible reason for this problem is that NDVI is not sensitive enough to the leaf-color change from green to yellow or red because green reflectance is not used in the calculation of NDVI. Meanwhile, there are a lot of spectral bands which can be measured by using remote sensing. Therefore, it is important to seek the applicability of various other spectral indices to develop the phenology detection with remote sensing.

In the study, we propose to use the Green-Red Vegetation Index (GRVI) [11,14]:

$$GRVI = \frac{\rho_{green} - \rho_{red}}{\rho_{green} + \rho_{red}} \quad (2)$$

where  $\rho_{green}$  is reflectance of visible green. We chose GRVI because the response of GRVI to various ground covers may be simple to interpret. In terms of the balance between green reflectance (wavelengths of around 500–570 nm) and red reflectance (wavelengths of around 620–700 nm), we can find three groups of spectral reflectance patterns for major components of ground cover (Figure 1):

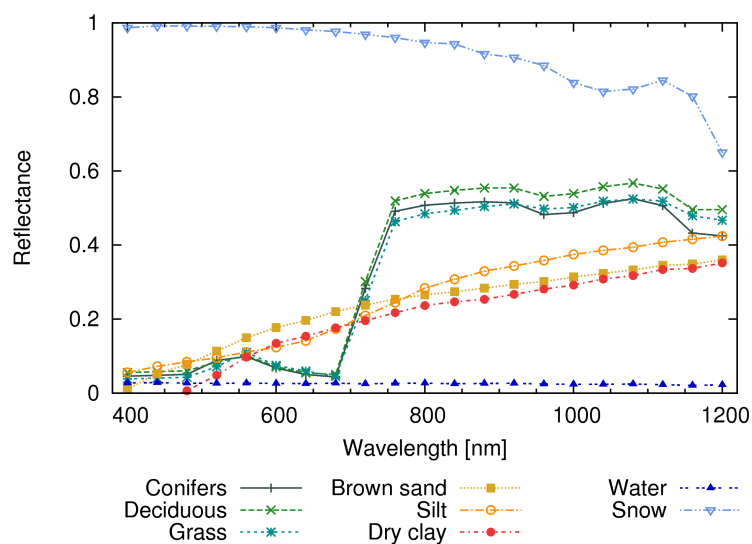
- Green vegetation (conifers, deciduous trees, and grass):  $\rho_{green}$  is higher than  $\rho_{red}$ .
- Soils (brown sand, silt, and dry clay):  $\rho_{green}$  is lower than  $\rho_{red}$ .
- Water/snow:  $\rho_{green}$  and  $\rho_{red}$  are mostly the same.

According to the Equation (2), green vegetation, soils, and water/snow have positive, negative, and near-zero values of GRVI, respectively. Therefore, we hypothesized that “GRVI = 0” becomes a effective threshold to distinguish between green vegetation and other types of the ground covers. Moreover, because the balance between green and red reflectance changes in response to leaf green-up and autumn coloring, the “GRVI = 0” threshold should be effective for phenology detection, too. Taking advantage of this feature, a simple algorithm for detecting the timing of leaf green-up and autumn coloring may be possible.

This idea can be verified with a time-series GRVI dataset with fine temporal resolution at various ecosystem types. However, few studies have used GRVI for ecological application (e.g., [16]), and the seasonal characteristics of GRVI are not well understood. Furthermore, to the best of the authors' knowledge, there have been no reports about leaf phenological changes being detected by GRVI.

The goal of this article is to evaluate GRVI as a phenological indicator. Based on an investigation of the relationships between GRVI values and the seasonal change of vegetation and ground surface, we discuss an effective method to detect phenological changes, especially leaf green-up and autumn coloring. To achieve our goal, we conducted multi-year stand-level ground observations of spectral reflectance and phenology at several representative ecosystems in Japan.

**Figure 1.** Typical spectral reflectance of vegetation, soils, water, and snow. The original data were downloaded from the ASTER Spectral Library [15] (<http://speclib.jpl.nasa.gov/>).



## 2. Materials and Methods

### 2.1. Study Sites

Study sites were located in four major ecosystems in Japan: deciduous broadleaf forest (Takayama site: TKY), deciduous coniferous forest (Fuji-hokuroku site: FHK), grassland (Terrestrial Environment Research Center in the University of Tsukuba: TGF), and paddy field (Mase site: MSE). Table 1 summarizes features of these sites. The sites belong to the Phenological Eyes Network [17] (<http://www.pheno-eye.org/>) and the JapanFlux network (<http://www.japanflux.org/>). TKY and FHK also belong to the JaLTER network (<http://www.jalter.org/>).

### 2.2. Observation System

Spectral irradiance data and photographs of sky and canopy surface were taken periodically and automatically at each site by a typical Phenological Eyes Network system (e.g., [13,21,22]), which mainly consists of a Hemi-Spherical Spectro-Radiometer (HSSR) and an Automatic-capturing Digital

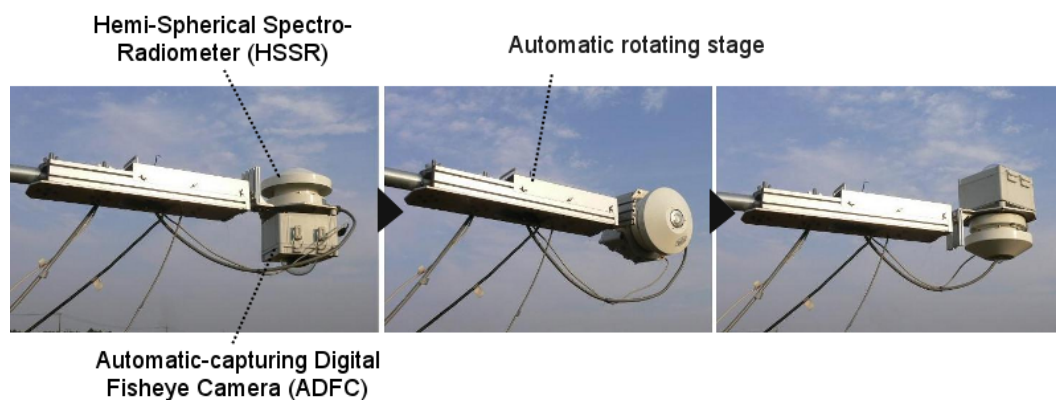
**Table 1.** The study sites.

	Takayama (TKY)	Fuji-hokuroku (FHK)	Univ. of Tsukuba (TGF)	Mase (MSE)
Location (WGS84)	36.1462 °N, 137.4231 °E	35.4436 °N, 138.7647 °E	36.1135 °N, 140.0949 °E	36.0539 °N, 140.0269 °E
Elevation (m.a.s.l.)	1420	1100	27	13
Mean annual air temperature, °C (period)	6.5 (1994–2005)	9.6 (2006–2007)	14.1 (2001–2003)	14.2 (2000–2007)
Mean annual precipitation, mm (period)	2275 (1980–2002)	1566 (2006-2-007)	1157 (2001–2003)	1318 (2000–2007)
Vegetation type	Deciduous broadleaf forest	Deciduous coniferous forest	Grassland (C3/C4 mixed)	Rice paddy field
Dominant species	Birch ( <i>Betula ermanii</i> ) Oak ( <i>Quercus crispula</i> ) Dwarf bamboo ( <i>Sasa senanensis</i> )	Japanese larch ( <i>Larix kaempferi</i> )	<i>Miscanthus sinensis</i> <i>Imperata cylindrica</i> <i>Solidago altissima</i>	<i>Oryza sativa L.</i> (cultivar: Koshihikari)
Canopy height, m	15–20	20–25	0–1.8	0–1.2
Annual maximum leaf area index	7.0 (trees and bamboos) [18]	2.8 (larch trees) *	5.6 [19]	6.3 [20]
Tower or mast height, m	18	32	3.0	2.4

\* Okano, T., unpublished data.

Fish-eye Camera (ADFC). Both HSSR and ADFC were installed atop a tower or a mast at each site. The HSSR measured the spectral irradiance of the sky and canopy, whereas the ADFC took photographs of the vegetation and the ground surface. Figure 2 shows a part of the system at the MSE site as an example. We analyzed the data taken in 2004–2008 at TKY, 2007 and 2008 at FHK, 2004 and 2008 at TGF, and 2005–2008 at MSE.

**Figure 2.** Observation system at MSE site: Hemi-Spherical Spectro-Radiometer (HSSR) and Automatic-capturing Digital Fish-eye Camera (ADFC) with automatic rotating stage.



## HSSR

At each site we used as the HSSR the MS-700 radiometer of EKO Instruments Co., Ltd. with a wavelength range of 350–1050 nm, wavelength interval of 3.3 nm, half-bandwidth of 10 nm, and wavelength accuracy of less than 0.3 nm; the HSSR was controlled by a personal computer (operating system: Microsoft Windows XP or Windows 2000) and software supplied with the MS-700 by the manufacturer.

At TKY, TGF, and MSE, we attached the MS-700 radiometer to an automatic rotating stage (CHS-AR, Hayasaka Rikoh Co., Ltd.), which can flip back and forth driven by an electric motor, enabling the HSSR to observe both downward and upward directions alternatively. The time lag of the nearest upward and downward measurements was 2 min. The rotating stage was also controlled by a personal computer

(operating system: Microsoft Windows XP or Windows 2000) and software supplied with the rotating stage by the manufacturer. We set the HSSR to observe both downward and upward directions every 10 min.

At FHK, we installed two HSSRs and did not use the rotating stage. Upward and downward spectral irradiance at the canopy top were measured simultaneously every 2 min by the two HSSRs. The instrumental error was corrected by comparing the data of downward spectral irradiance measured with the two HSSRs for several days from August to September each year.

#### ADFC

We used a CoolPix-4300 or a CoolPix-4500 digital cameras (Nikon Corporation), both with a fish-eye lens FC-E8 (Nikon Corporation), as the ADFC. Each camera was stored in a custom-built housing SPC31A (Hayasaka Rikoh Co., Ltd.). At TKY, FHK, and TGF, we installed downward and upward cameras at the end of a horizontal iron pipe attached to the tower top. At MSE, we attached a camera to the rotating stage on the backside of the HSSR. Upward (sky) photographs were used for checking the weather condition for quality control of the spectral data. Downward (canopy) photographs were used for monitoring seasonal change of vegetation and ground condition. To control the functions of the cameras (such as parameter configuration, image capture, and data retrieval), we used the free software “photopc” (<http://photopc.sourceforge.net/>) on the personal computers (operating system: Microsoft Windows XP, Windows 2000, or Linux). The configuration of the cameras was as follows: mode, programmed auto; white balance, Sunny or Auto; image size,  $2272 \times 1704$  pixels; fisheye mode, Fisheye-1 (circular); file format, JPEG. We set the cameras to capture the sky every 2 min (TKY and TGF), 10 min (FHK), and 5 min (MSE), and to capture the vegetation and the ground every 90 min (TKY), 60 min (FHK), and 30 min (TGF and MSE).

#### 2.3. Calculation of Spectral Indices

Daily spectral indices were calculated from the ground-measured spectral irradiance as follows:

1. The ground-measured spectral irradiances were converted to band-averaged irradiances by using the relative spectral response function of band 1 (visible red; wavelength 620–670 nm), band 2 (near-infrared; wavelength 841–876 nm), and band 4 (visible green; wavelength 545–565 nm) of the MODIS sensor on NASA’s Terra satellite (e.g., [23]; [ftp://ftp.mcst.ssai.biz/pub/permanent/MCST/PFM\\_L1B\\_LUT\\_4-30-99/](ftp://ftp.mcst.ssai.biz/pub/permanent/MCST/PFM_L1B_LUT_4-30-99/)).
2. Daily band-averaged irradiances were obtained by averaging the band-averaged irradiances measured from 10:00 to 14:00 each day.
3. Daily band-averaged reflectances were obtained by dividing the daily band-averaged irradiances of the ground by that of the sky.
4. Daily spectral indices (GRVI and NDVI) were calculated from the daily band-averaged reflectances by using Equations (1) and (2).

5. By reference to the ADFC images, data taken under rainy conditions were discarded, and only data collected under sunny or cloudy conditions were used for analysis.

### 3. Results

#### 3.1. TKY Site: Deciduous Broadleaf Forest

At TKY, according to the ADFC images, the ground was covered with snow approximately from day of year (DOY) 350 to DOY 90. The snow-melt occurred approximately between DOY 90 and 120, but the exact timing varied from year to year. The green-up of canopy species started on approximately DOY 140. The autumn leaf coloring started on approximately DOY 270. Birch trees (*Betula ermanii*) showed autumn coloring earlier than oak trees (*Quercus crispula*). Most trees were defoliated by approximately DOY 310.

During the snow period from 2004 to 2008 at TKY, GRVI was about zero and NDVI was about 0.1; during the snow-melt period, GRVI decreased but NDVI increased (Figure 3, DOY 90–120). When the snow disappeared completely (on DOY 120), GRVI was approximately  $-0.1$ , while NDVI was approximately 0.4, which was nearly at the middle of the annual range of NDVI. Although the temporal change of each index was smooth during this snow-melt period, we observed sudden increase and decrease from DOY 110 to 112 in 2006; this spike was associated with a temporal snow cover.

When the canopy trees started to grow leaves (leaf green-up), GRVI and NDVI started to increase rapidly (on DOY 140). GRVI turned from negative to positive values at the beginning of leaf green-up (see photograph 2007-144 in Figure 3). By approximately DOY 150, most of the canopy was covered with bright-green leaves, and GRVI and NDVI stopped increasing at this time and reached the annual maximum level of approximately 0.35 and 0.9, respectively (Table 2). After that, GRVI gradually decreased as the leaves gradually turned dark green, while NDVI remained nearly constant.

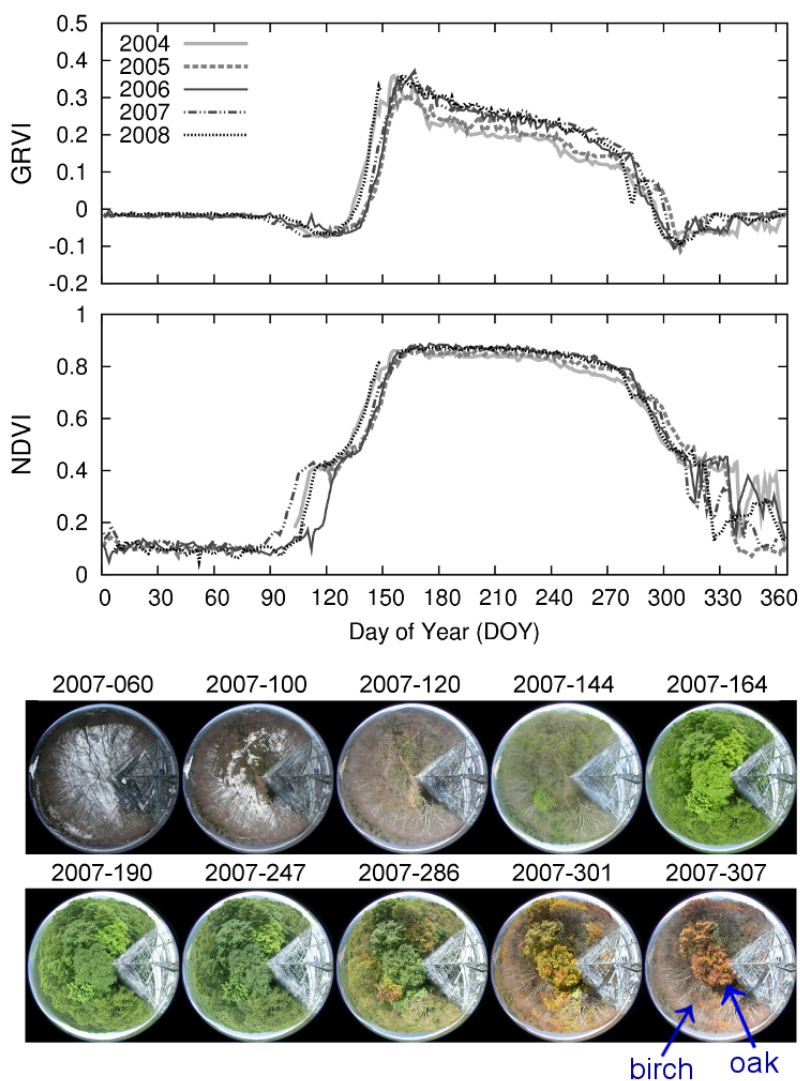
In 2004, big typhoons hit the TKY site on DOY 173 (typhoon Dianmu) and 244 (typhoon Chaba). As a consequence, many green leaves dropped from the canopy, and GRVI sharply decreased, which is unusual during the growing period. Meanwhile, NDVI did not change in response to these typhoons.

GRVI and NDVI rapidly decreased when the leaves turned yellow or red (DOY 270–310). GRVI shifted from positive to negative values at the middle of the autumn coloring period (see photograph

**Table 2.** Annual maximum and minimum values of GRVI and NDVI at TKY sites.

Year	GRVI		NDVI	
	Annual maximum	Annual minimum	Annual maximum	Annual minimum
2004	0.359 (DOY 165)	$-0.097$ (DOY 306)	0.877 (DOY 175)	0.096 (DOY 4)
2005	0.310 (DOY 164)	$-0.112$ (DOY 309)	0.871 (DOY 202)	0.068 (DOY 41)
2006	0.359 (DOY 165)	$-0.101$ (DOY 306)	0.888 (DOY 175)	0.048 (DOY 4)
2007	0.371 (DOY 167)	$-0.111$ (DOY 306)	0.881 (DOY 178)	0.086 (DOY 80)
2008	0.361 (DOY 160)	$-0.097$ (DOY 309)	0.877 (DOY 183)	0.050 (DOY 52)

**Figure 3.** Annual cycle of ground-measured spectral indices and canopy images from the Takayama site (TKY: deciduous broadleaf forest). The graphs show time-series GRVI and NDVI observed by the HSSR from 2004 to 2008. The photographs show the typical condition of each stage of the annual cycle in 2007. The date of each photograph is denoted at the top as “year”–“day-of-year”. The oak trees are at the center of the photographs, and the birch trees surround the center.

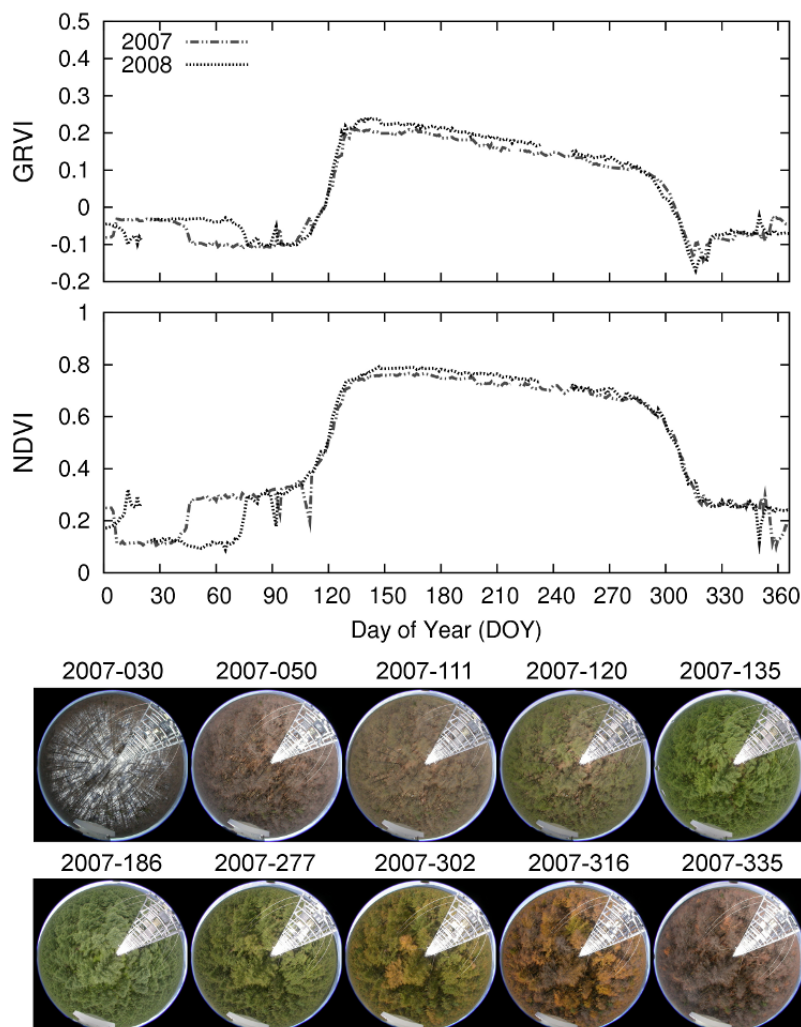


2007-301 in Figure 3). When the canopy turned bright red (see photograph 2007-307 in Figure 3), GRVI declined to the annual minimum value which is shown in Table 2.

### 3.2. FHK Site: Deciduous Coniferous Forest

According to the ADFC images, the ground at FHK was covered with snow in January and February. The snow-melt occurred by approximately DOY 40 in 2007 and by approximately DOY 70 in 2008. When the snow had disappeared completely, the forest floor was not covered with green leaves. The green-up of the larch trees started on approximately DOY 110. The larch canopy became covered with

**Figure 4.** Annual cycle of ground-measured spectral indices and canopy images from the Fuji-hokuroku site (FHK: deciduous coniferous forest). The graphs show time-series GRVI and NDVI observed by the HSSR in 2007 and 2008. The photographs show the typical condition of each stage of the annual cycle in year 2007. The date of each photograph is denoted at the top as "year"–"day-of-year".



bright-green leaves by approximately DOY 135. The leaves turned to yellow and red from DOY 280, and most leaves had dropped by approximately DOY 320.

During the snow period in year 2007 to 2008 at FHK, GRVI was approximately zero and NDVI was approximately 0.1 (Figure 4, DOY 30); during the snow-melt period, GRVI increased and NDVI decreased (Figure 4, on approximately DOY 40 in 2007, DOY 70 in 2008). When the snow disappeared, GRVI was approximately  $-0.1$ , while NDVI was approximately 0.3. Temporary snowfall and snow-melt occurred on DOY 93 and 109 in 2007, and DOY 91 in 2008, resulting in the short-term spike-like changes in GRVI and NDVI.

GRVI and NDVI rapidly increased just after the canopy species started to grow leaves (DOY 110–130). GRVI turned from negative to positive values as soon as the leaf green-up started (see photograph 2007-120 in Figure 4). When leaves covered much of the canopy (see photograph

**Table 3.** Annual maximum and minimum values of GRVI and NDVI at FHK sites.

Year	GRVI		NDVI	
	Annual maximum	Annual minimum	Annual maximum	Annual minimum
2007	0.211 (DOY 133)	-0.144 (DOY 320)	0.767 (DOY 163)	0.101 (DOY 359)
2008	0.242 (DOY 142)	-0.170 (DOY 316)	0.792 (DOY 147)	0.088 (DOY 065)

2007-135 in Figure 4), GRVI and NDVI stopped increasing and reached the annual maximum level of approximately 0.2 and 0.8, respectively (Table 3). Subsequently, GRVI gradually decreased, while NDVI maintained the maximum level for at least one month more.

When the leaves turned yellow and red, both GRVI and NDVI rapidly decreased (DOY 280–320). GRVI turned from positive to negative during the middle of this period (see photograph 2007-302 in Figure 4). When the canopy color became bright red (see photograph 2007-316 in Figure 4), GRVI reached the annual minimum value which is shown in Table 3.

### 3.3. TGF Site: Grassland

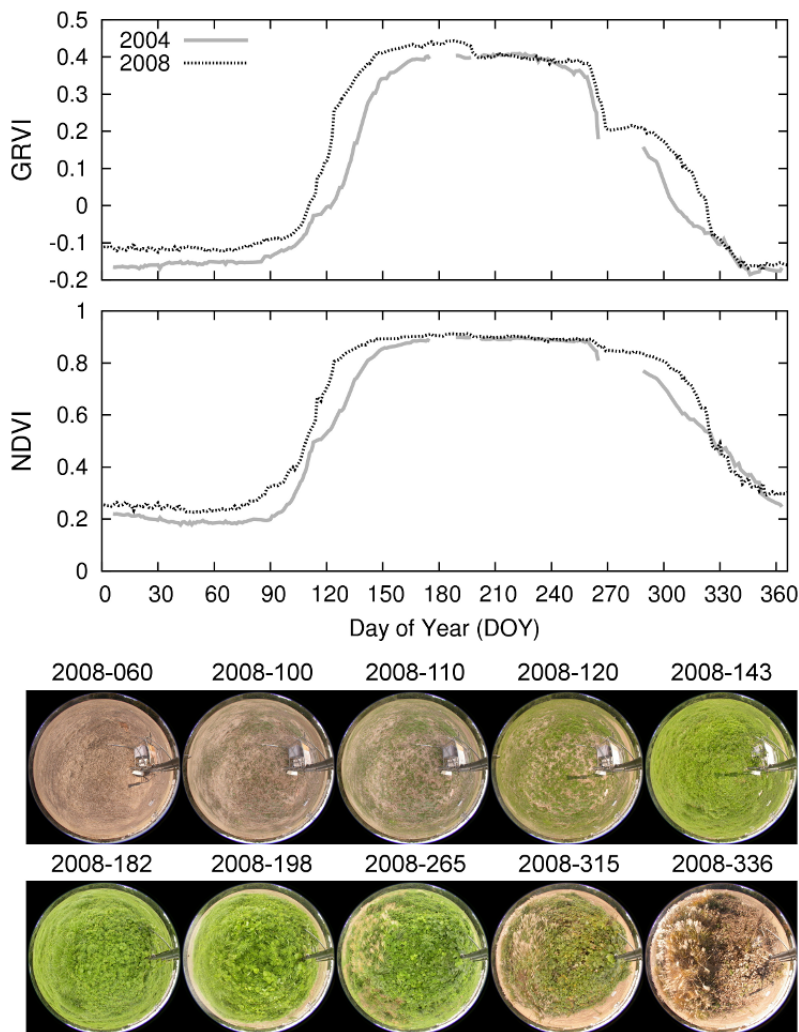
According to the ADFC images, bare soil and withered plants covered much of the ground at TGF from DOY 340 to 90. Emergence of the aerial parts of grasses started on approximately DOY 100 in both 2004 and 2008. The ground was almost covered with leaves by approximately DOY 150. The flowering and heading of the plants started on approximately DOY 265. After that, the plants gradually withered and became yellow. Most plants had withered by approximately DOY 330. In 2004, withered plants were mown down on DOY 351.

During the non-growing period of the grasses at TGF in 2004 and 2008, GRVI was negative (between -0.2 and -0.1) and NDVI was approximately 0.2 (Figure 5, DOY 340–90). After the emergence of the green leaves, GRVI and NDVI increased sharply with increasing vegetation cover. When the ground was almost covered with green leaves (see photograph 2008-143 in Figure 5), GRVI and NDVI stopped increasing and reached the annual maximum level of approximately 0.4 and 0.9, respectively (Table 4). From DOY 150 to 270, GRVI and NDVI remained approximately constant, but GRVI slightly decreased when the aerial parts in the corners of the observation range were mown down (see photograph 2008-198 in Figure 5). The decrease of approximately 20 percent of green grass cover, which was estimated by a visual interpretation of the ADFC photos, was corresponding to approximately 7 percent decrease in GRVI. Meanwhile, NDVI did not change in response to this green cover decrease.

**Table 4.** Annual maximum and minimum values of GRVI and NDVI at TGF sites.

Year	GRVI		NDVI	
	Annual maximum	Annual minimum	Annual maximum	Annual minimum
2004	0.444 (DOY 188)	-0.173 (DOY 353)	0.914 (DOY 194)	0.226 (DOY 49)
2008	0.409 (DOY 223)	-0.185 (DOY 346)	0.899 (DOY 192)	0.178 (DOY 42)

**Figure 5.** Annual cycle of ground-measured spectral indices and canopy images from the Terrestrial Environment Research Center in the University of Tsukuba (TGF: grassland). The graphs show time-series GRVI and NDVI observed by the HSSR in 2004 and 2008. The photographs show the typical condition of each stage of the annual cycle in year 2008. The date of each photograph is denoted at the top as “year”—“day-of-year”.



GRVI rapidly decreased by half in response to the flowering and heading on approximately DOY 265; in contrast, NDVI slightly decreased. When the plants turned yellow, both GRVI and NDVI decreased. GRVI became negative during this period (see photograph 2008-315 in Figure 5).

#### 3.4. MSE Site: Paddy Field

According to ADFC images, the ground at the MSE was covered with bare soil from DOY 320 to 110. The field was irrigated from approximately DOY 110. Rice plants were transplanted on approximately DOY 120 each year. Agricultural machines planted seedlings at approximately 30 cm intervals. Heading of rice plants occurred by approximately DOY 200; after that, the rice plants gradually changed to yellow.

The aerial parts were harvested between DOY 250 and 270. After harvest, ratoons grew from the crowns of the residual rice plants.

During the non-growing period from 2005 to 2008, GRVI was negative (approximately  $-0.1$ ) and NDVI was approximately  $0.2$  (Figure 6, DOY 320–110). GRVI and NDVI showed a small spike-like change on DOY 34 in 2008 associated with a temporal snow cover. After irrigation (see photograph 2007-117 in Figure 6), GRVI sharply increased to approximately  $-0.05$  and NDVI sharply decreased to approximately  $0.1$ .

**Figure 6.** Annual cycle of ground-measured spectral indices and canopy images from the Mase site (MSE: paddy field). The graphs show time-series GRVI and NDVI observed by the HSSR from 2005 to 2008. The photographs show the typical condition of each stage of the annual cycle in year 2007. The date of each photograph is denoted at the top as “year”–“day-of-year”. The white spot which is seen in the fisheye photographs on 2007-117, 132, and 153 is a sun glint.

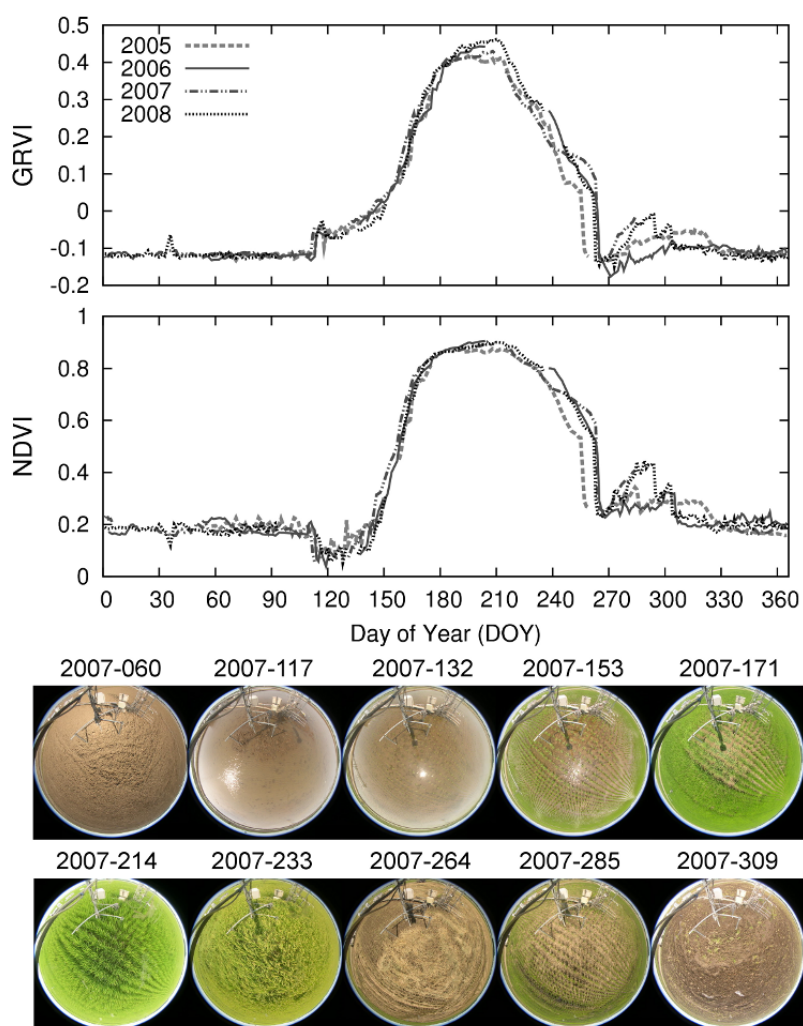


**Table 5.** Annual maximum and minimum values of GRVI and NDVI at MSE sites.

Year	GRVI		NDVI	
	Annual maximum	Annual minimum	Annual maximum	Annual minimum
2005	0.417 (DOY 195)	-0.134 (DOY 269)	0.876 (DOY 208)	0.073 (DOY 115)
2006	0.443 (DOY 201)	-0.176 (DOY 271)	0.905 (DOY 204)	0.039 (DOY 119)
2007	0.430 (DOY 208)	-0.136 (DOY 268)	0.901 (DOY 205)	0.054 (DOY 113)
2008	0.462 (DOY 210)	-0.150 (DOY 273)	0.901 (DOY 211)	0.053 (DOY 128)

Both GRVI and NDVI increased from approximately one month after rice transplanting. The increases in GRVI and NDVI stopped on approximately DOY 200, and GRVI and NDVI reached the annual maximum level of approximately 0.4 and 0.9, respectively (Table 5).

Both GRVI and NDVI decreased after the rice plants headed (see photograph 2007-214 in Figure 6). Just after harvest (see photograph 2007-264 in Figure 6), GRVI and NDVI had sharply decreased, and GRVI shifted to negative values. For approximately one month after harvest, GRVI and NDVI increased slightly with ratoon growth (see photograph 2007-285 in Figure 6).

### 3.5. Summary of the Relationships Between the Spectral Indices and the Condition of the Sites

Figure 7 summarizes the relationships between the spectral indices and the condition of the vegetation and ground at the four study sites. In Figure 7, we classified the conditions of sites into the six categories based on the visual interpretation of the daily ADFC images (Table 6). For TKY and FHK sites, we defined the categories as follows: “green leaf” period was the period when the dominant canopy trees (birch and oak for TKY; larch for FHK; see Table 1) in a image were expanding their green leaves; “yellow/red leaf” period was the period from when the dominant canopy trees began to turn yellow until the end of defoliation; “snow cover” period was the period when the ground was covered with snow including snow-melt period; the other periods except the days with temporal snow cover were defined as “understory vegetation with leafless trees”. For TGF site, “green leaf” period was the period when more than 20 percent of the ground was covered with green leaves of grass plants; “yellow/red leaf” period was the period from the heading and flowering until the mowing of an aerial part of plants; the other periods except the days with temporal snow cover were defined as “bare soil”. For MSE site, “green leaf” period was the period from the transplanting of seedlings until the heading; “yellow/red leaf” period was the same definition as TGF site; “irrigation water” period was the period when the ground was covered with water but the rice plants were not transplanted; the other periods except the days with temporal snow cover were defined as “bare soil”. We chose the start and end dates of each category so that the conditions of the vegetation and the ground in ADFC images were same among years as much as possible.

At all the sites, GRVI was positive during most of the growing period (mainly green-leaf period), negative when plants had no leaves, and approximately zero with snow and irrigation water. GRVI was also near zero with understory vegetation and leafless trees.

NDVI was positive during the entire period. The minimum NDVI values of the green-leaf category varied widely among the sites. It was caused by the different NDVI values of each site at the start of

leaf green-up period. Unlike GRVI, NDVI of understory vegetation was higher than that of snow and irrigation water.

**Figure 7.** The range of (a) GRVI and (b) NDVI values for the representative conditions of the sites. We classified the conditions of sites into the six categories based on the visual interpretation of the daily ADFC images (see subsection 3.5 and Table 6).

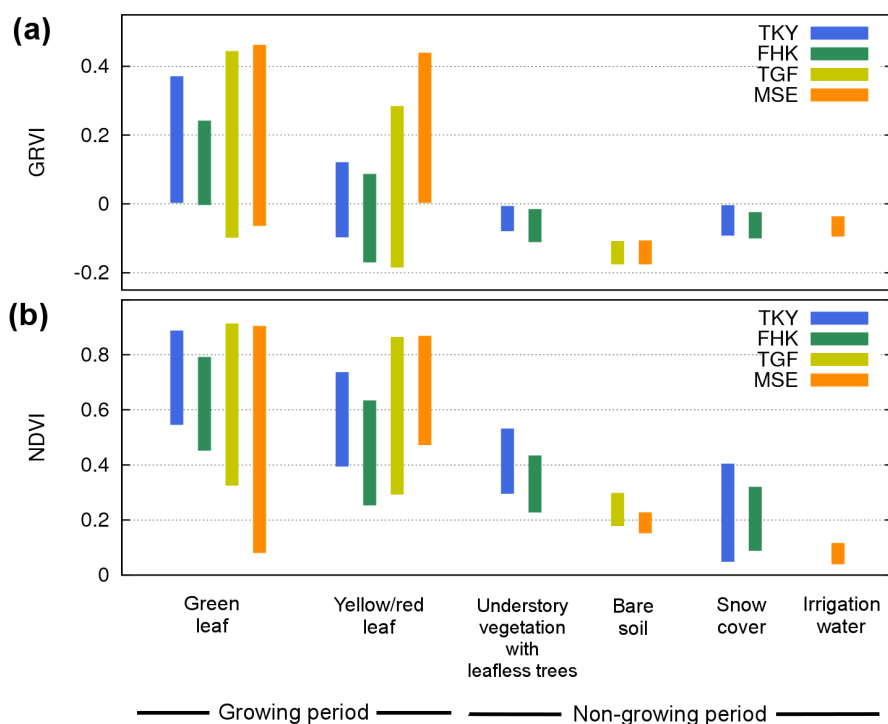


**Table 6.** The start and end DOYs of each category in Figure 7.

		Green leaf	Yellow/red leaf	Understory vegetation with leafless trees	Bare soil	Snow cover	Irrigation water
TKY	2004	134–282	283–309	111–134, 310–340	-	103–110* <sup>1</sup> , 341–366	-
	2005	141–284	285–315	118–140* <sup>2</sup> , 316–333	-	1–108* <sup>2</sup> , 334–365	-
	2006	142–282	283–310	126–141, 311–335	-	1–125, 336–365	-
	2007	142–285	286–313	111–141, 314–315	-	1–110, 316–365	-
	2008	134–274	275–312	115–133, 313–323	-	1–114, 324–366	-
FHK	2007	117–292	293–324	1–5, 46–116, 325–356	-	6–45, 357–366	-
	2008	115–285	286–324	12–20, 82–114, 325–366	-	1–11, 21–75, 349–352	-
TGF	2004	104–259	260–351	-	1–103, 352–366	-	-
	2008	105–263	264–366	-	1–108	-	-
MSE	2005	122–214	215–259	-	65–113* <sup>3</sup> , 330–365	-	114–121
	2006	122–206* <sup>4</sup>	237–264* <sup>4</sup>	-	1–113, 332–365	-	114–121
	2007	123–215	216–263	-	1–111, 302–365	-	112–120
	2008	123–214	215–262	-	1–113* <sup>5</sup>	-	114–122

\*<sup>1</sup> The measurements were started on DOY 103.

\*<sup>2</sup> HSSR and ADFC data were missing from DOY 109 to DOY 117.

\*<sup>3</sup> The measurements were started on DOY 65.

\*<sup>4</sup> HSSR and ADFC data were missing from DOY 207 to DOY 236.

\*<sup>5</sup> Canopy ADFC images were missing from DOY 275 to DOY 366.

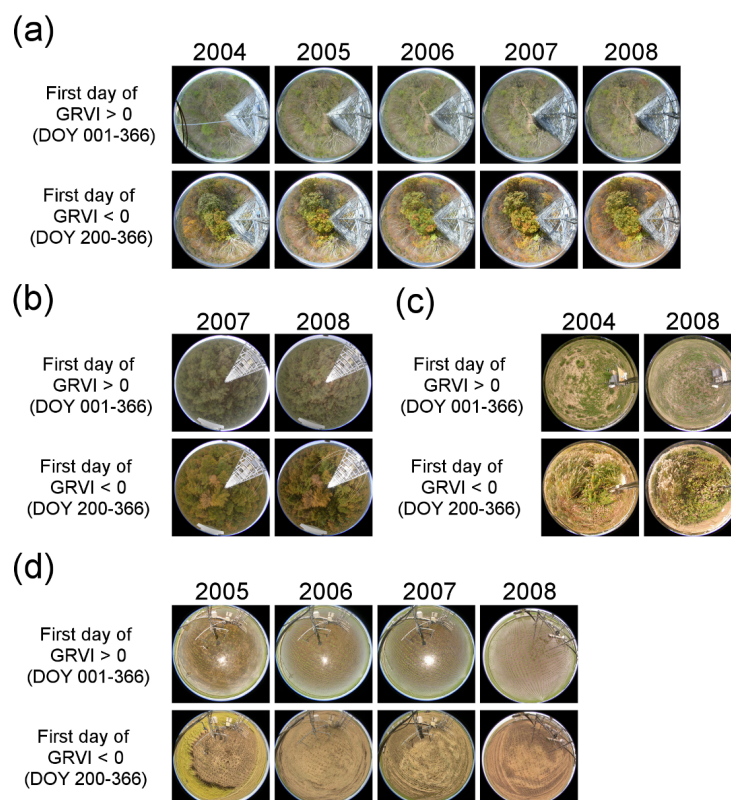
#### 4. Discussion

##### 4.1. Applicability of GRVI as an Indicator of Vegetation Phenology

Our results suggest that “GRVI = 0” can be a simple and clear threshold that discriminates the period when the canopy was covered with green leaves from the period with the other conditions (*i.e.*, bare soil, snow cover, water). This result supported our hypothesis about GRVI behavior mentioned in the introduction. The canopy photographs taken on the first day each year when GRVI had increased above zero show the early phase of leaf green-up; the photographs taken on the first day each year after DOY 200 when GRVI had declined to less than zero show the middle phase of autumn coloring at the TKY, FHK, and TGF site (Figure 8). At the MSE site (paddy field), the first GRVI > 0 photographs show approximately 20 days after transplanting, and the latter GRVI < 0 photographs show just after harvest. Figure 8 also shows that the vegetation condition indicated by “GRVI = 0” was consistent among years in each site. These site-independent and year-independent features are useful to make a simple algorithm of phenology detection using remote sensing.

Such clear and site-independent features were absent in the NDVI data. According to Figure 7, the NDVI value at the start of green-leaf period had a big difference among the sites. In particular, the NDVI values for the growing period and the NDVI values of snow cover and understory vegetation

**Figure 8.** Canopy-top photographs on the first day of the year when “GRVI > 0” and the first day of “GRVI < 0” from DOY 200 to 366 in each year at (a) TKY (deciduous broadleaf forest), (b) FHK (deciduous coniferous forest), (c) TGF (grassland), and (d) MSE (paddy field).



somewhat overlapped. Therefore, NDVI cannot clearly discriminate the growing period from other conditions with a simple site-independent single threshold. We must consider the presence or absence of snow/water cover and understory vegetation for each target when we use NDVI, as pointed out by several studies [24–27]. Furthermore, as Nagai *et al.* [13] have reported, the canopy condition of autumn coloring corresponded to different NDVI values from year to year. These results suggest that a single NDVI threshold cannot offer us to detect the vegetation phenology with a simple and stable algorithm. However, this study tested only the phenology detection by a single threshold of NDVI, and there are several other methods such as the use of an annual half-maximum value [8], an inflection point [6], and a maximum rate of curvature [28]. Hence, additional work is needed to evaluate the performance of the phenology detection using NDVI completely.

GRVI is an effective indicator particularly for autumn coloring of leaves. “GRVI = 0” can be a threshold for detecting the middle phase of autumn coloring as noted above, and in addition, the annual minimum of GRVI corresponded with the late stage of autumn coloring (the leaves turn bright red) at the forest sites TKY and FHK. Such a clear correspondence between the late stage of autumn coloring and NDVI data was not apparent (Figure 3 and Table 2 for TKY; Figure 4 and Table 3 for FHK). The better correspondence between GRVI and autumn phenological changes is because GRVI is, in principle, sensitive to change in visible colors of the canopy.

One limitation of GRVI as a phenological indicator is that GRVI cannot detect the timing of transplanting of rice in paddy fields because GRVI showed few changes shortly after transplanting. The same thing was seen in NDVI as well. This is, in part, because the coverage by the rice plants just after transplanting is too small.

#### 4.2. Other Advantages of GRVI as an Ecosystem Indicator

GRVI decreased in response to the changes in canopy vegetation even in the middle of the growing period when the apparent change of leaf colors and leaf density were small. For example, as seen in the results for TKY and TGF, GRVI decreased in response to leaf fall by typhoons, mowing of plants, and flowering/heading of grass plants. According to Figure 9, which shows the relative value of GRVI and NDVI, GRVI kept changing during the entire growing period, whereas NDVI stopped changing in the middle of the growing period at a saturation value. This suggests that GRVI is better for detecting subtle disturbance in the middle of the growing period.

The GRVI data clearly correspond with different patterns of seasonal change among ecosystem types: namely, between deciduous forests and grassland. At the TKY site (deciduous forest), the graph of DOY *versus* GRVI showed an asymmetric pattern: a rapid increase up to the peak and a slow decrease after the peak (Figure 9). At the TGF site (grassland), the graphs were symmetric and bell-shaped (Figure 9). In contrast, the graphs of NDVI were almost symmetric and bell-shaped at each site, and it is difficult to distinguish between the TKY site and the TGF site by the seasonal pattern of NDVI. Therefore, the seasonal pattern of GRVI can be utilized to classify ecosystem types, especially deciduous forest and grassland. This may be because GRVI is sensitive to changes in green color. After the canopy leaves covered most of the ground (canopy closing), the temporal change of red reflectance (corresponding to MODIS band-1) was so little that we could not find any site-dependant features (Figure 10). However, in that period, the green reflectance (corresponding to MODIS band-4) showed

unique characteristic behavior at each site, in particular, between the deciduous forest sites (TKY and FHK) and the herbaceous sites (TGF and MSE): green reflectance gradually decreased at TKY and FHK, whereas the green reflectance remained almost constant at TGF and MSE. Light absorption of

**Figure 9.** Relative value of GRVI and NDVI during the growing period at each site. The relative value were calculated by using the following equation: relative value of spectral indices =  $(N - N_{min}) / (N_{max} - N_{min})$ , where  $N$ ,  $N_{max}$  and  $N_{min}$  represents the daily spectral indices, the annual maximum spectral indices, and the annual minimum spectral indices, respectively.

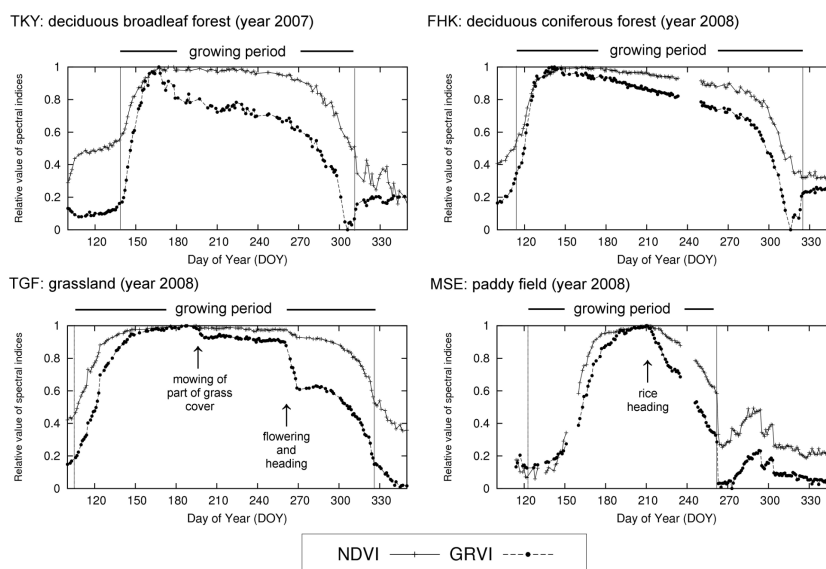
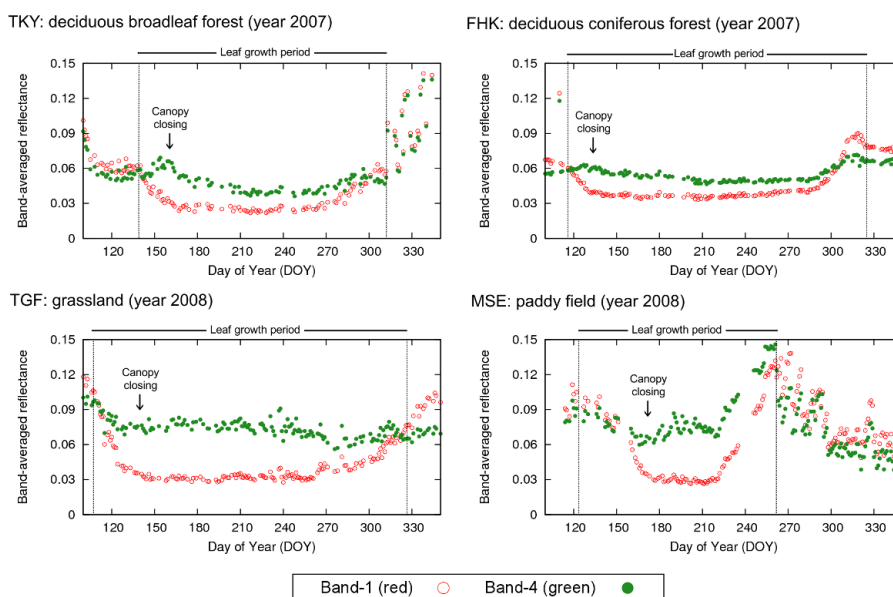


**Figure 10.** Time series of band-averaged reflectance (Terra MODIS bands 1 and 4) observed by the HSSR during the growing period at each site. “Canopy closing” represents the day when leaves almost covered the canopy.



the vegetation canopy mainly depends on leaf growth processes and spatial layout; hence, the seasonal change of green reflectance could represent leaf development patterns of each ecosystem.

In conclusion, our data suggested that GRVI is a useful indicator of not only vegetation phenology especially for leaf autumn coloring, but also disturbance and ecosystem types. Although this study demonstrates the utility of GRVI by using datasets at the four types of vegetation, additional research is obviously needed to evaluate our findings at various sites around the world.

### Acknowledgements

We thank Shin Nagai (Japan Agency for Marine-Earth Science and Technology); Hiroyuki Muraoka (Gifu University, Japan); Nobuko Saigusa and Reiko Ide (National Institute for Environmental Studies, Japan); and Akira Miyata, Masayoshi Mano, and Keisuke Ono (National Institute for Agro-Environmental Sciences, Japan) for supporting our field work. The data of leaf area index of FHK site was provided by Tetsuo Okano (Shinshu University, Japan). This study was supported by a Grant-in-Aid for JSPS Fellows from Japan Society for the Promotion of Science (08J1376), a Grant-in-Aid for Young Scientists from The Ministry of Education, Culture, Sports, Science and Technology in Japan (19088012), JSPS-NRF-NSFC A3 Foresight Program (quantifying and predicting terrestrial carbon sinks in East Asia: toward a network of climate change research), and a Global Change Observation Mission (GCOM; PI#102) of the Japan Aerospace Exploration Agency (JAXA).

### References

1. Cleland, E.E.; Chuine, I.; Menzel, A.; Mooney, H.A.; Schwartz, M.D. Shifting plant phenology in response to global change. *Trends Ecol. Evol.* **2007**, *22*, 357-365.
2. Myneni, R.B.; Keeling, C.D.; Tucker, C.J.; Asrar, G.; Nemani, R.R. Increased plant growth in the northern high latitudes from 1981 to 1991. *Nature* **1997**, *386*, 698-702.
3. Tucker, C.J.; Slayback, D.A.; Pinzon, J.E.; Los, S.O.; Myneni, R.B.; Taylor, M.G. Higher northern latitude normalized difference vegetation index and growing season trends from 1982 to 1999. *Int. J. Biometeorol.* **2001**, *45*, 184-190.
4. Stöckli, R.; Vidale, P.L. European plant phenology and climate as seen in a 20 year AVHRR land-surface parameter dataset. *Int. J. Remote Sens.* **2004**, *25*, 3303-3330.
5. Delbart, N.; Le Toan, T.; Kergoat, L.; Fedotova, F. Remote sensing of spring phenology in boreal regions: A free of snow-effect method using NOAA-AVHRR and SPOT-VGT data (1982-2004). *Remote Sens. Environ.* **2006**, *101*, 52-62.
6. Piao, S.; Fang, J.; Zhou, L.; Ciais, P.; Zhu, B. Variations in satellite-derived phenology in China's temperate vegetation. *Global Change Biol.* **2006**, *12*, 672-685.
7. Karlsen, S.R.; Høgda, K.A.; Wielgolaski, F.E.; Tolvanen, A.; Tømmervik, H.; Poikolainen, J.; Kubin, E. Growing-season trends in fennoscandia 1982–2006, determined from satellite and phenology data. *Clim. Res.* **2009**, *39*, 275-286.
8. White, M.A.; Thornton, P.E.; Running, S.W. A continental phenology model for monitoring vegetation responses to interannual climatic variability. *Global Biogeochem. Cycles* **1997**, *11*, 217-234.

9. Botta, A.; Viovy, N.; Ciais, P.; Friedlingstein, P.; Monfray, P. A global prognostic scheme of leaf onset using satellite data. *Global Change Biol.* **2000**, *6*, 709-725.
10. Bradley, B.A.; Mustard, J.F. Comparison of phenology trends by land cover class: A case study in the Great Basin, USA. *Global Change Biol.* **2008**, *14*, 334-346.
11. Tucker, C.J. Red and photographic infrared linear combinations for monitoring vegetation. *Remote Sens. Environ.* **1979**, *8*, 127-150.
12. Pettorelli, N.; Vik, J.O.; Mysterud, A.; Gaillard, J.M.; Tucker, C.J.; Stenseth, N.C. Using the satellite-derived NDVI to assess ecological responses to environmental change. *Trends Ecol. Evol.* **2005**, *20*, 503-510.
13. Nagai, S.; Nasahara, K.N.; Muraoka, H.; Akiyama, T.; Tsuchida, S. Field experiments to test the use of the normalized difference vegetation index for phenology detection. *Agric. Forest Meteorol.* **2010**, *150*, 152-160.
14. Falkowski, M.J.; Gessler, P.E.; Morgan, P.; Hudak, A.T.; Smith, A.M.S. Characterizing and mapping forest fire fuels using ASTER imagery and gradient modeling. *Forest Ecol. Manage.* **2005**, *217*, 129-146.
15. Baldridge, A.M.; Hook, S.J.; Grove, C.I.; Rivera, G. The ASTER spectral library version 2.0. *Remote Sens. Environ.* **2008**, *113*, 711-715.
16. Coops, N.C.; Johnson, M.; Wulder, M.A.; White, J.C. Assessment of QuickBird high spatial resolution imagery to detect red attack damage due to mountain pine beetle infestation. *Remote Sens. Environ.* **2006**, *103*, 67-80.
17. Nishida, K. Phenological Eyes Network (PEN)—A validation network for remote sensing of the terrestrial ecosystems. *AsiaFlux Newslett.* **2007**, *21*, 9-13.
18. Nasahara, K.N.; Muraoka, H.; Nagai, S.; Mikami, H. Vertical integration of leaf area index in a Japanese deciduous broad-leaved forest. *Agric. Forest Meteorol.* **2008**, *148*, 1136-1146.
19. Nishida, K.; Higuchi, A. Seasonal change of grassland vegetation found in the preliminary GLI experiment in the Environmental Research Center. *Bull. Terrestrial Environ. Res. Center, Univ. Tsukuba* **2001**, *1*, 1-10, (in Japanese).
20. Saito, M.; Miyata, A.; Nagai, H.; Yamada, T. Seasonal variation of carbon dioxide exchange in rice paddy field in Japan. *Agric. Forest Meteorol.* **2005**, *135*, 93-109.
21. Motohka, T.; Nasahara, K.N.; Miyata, A.; Mano, M.; Tsuchida, S. Evaluation of optical satellite remote sensing for rice paddy phenology in monsoon Asia using continuous *in-situ* dataset. *Int. J. Remote Sens.* **2009**, *30*, 4343-4357.
22. Nagai, S.; Saigusa, N.; Muraoka, H.; Nasahara, K.N. What makes the satellite-based EVI-GPP relationship unclear in a deciduous broad-leaved forest? *Ecol. Res.* **2010**, *25*, 359-365.
23. Dall'Olmo, G.; Gitelson, A.A.; Rundquist, D.C.; Leavitt, B.; Barrow, T.; Holz, J.C. Assessing the potential of SeaWiFS and MODIS for estimating chlorophyll concentration in turbid productive waters using red and near-infrared bands. *Remote Sens. Environ.* **2005**, *96*, 176-187.
24. Moulin, S.; Kergoat, L.; Viovy, N.; Dedieu, G. Global scale assessment of vegetation phenology using NOAA/AVHRR satellite measurements. *J. Clim.* **1997**, *10*, 1154-1170.
25. Schwartz, M.D.; Reed, B.C. Surface phenology and satellite sensor-derived onset of greenness: An initial comparison. *Int. J. Remote Sens.* **1999**, *20*, 3451-3457.

26. Suzuki, R.; Nomaki, T.; Yasunari, T. West-east contrast of phenology and climate in northern Asia revealed using a remotely sensed vegetation index. *Int. J. Biometeorol.* **2003**, *47*, 126-138.
27. Delbart, N.; Kergoat, L.; Le Toan, T.; L'Hermitte, J.; Picard, G. Determination of phenological dates in boreal regions using Normalised Difference Water Index. *Remote Sens. Environ.* **2005**, *97*, 26-38.
28. Zhang, X.; Friedl, M.A.; Schaaf, C.B.; Strahler, A.H.; Hodges, J.C.F.; Gao, F.; Reed, B.C.; Huete, A. Monitoring vegetation phenology using MODIS. *Remote Sens. Environ.* **2003**, *84*, 471-475.

© 2010 by the authors; licensee MDPI, Basel, Switzerland. This article is an open access article distributed under the terms and conditions of the Creative Commons Attribution license (<http://creativecommons.org/licenses/by/3.0/>.)